AIAA JOURNAL
Vol. 31, No. 2, February 1993

Hysteresis Effects on Wind Tunnel Measurements of a Two-Element Airfoil

Kasim Biber* and Glen W. Zumwalt†
Wichita State University, Wichita, Kansas 67260

Wind-tunnel tests were conducted on the GA(W)-2 airfoil with 25%-slotted flap at Reynolds number of 2.2×10^6 and Mach number of 0.13. The tests were made for flap nested and flap deflected cases of 30 and 40 deg with optimum and narrow gaps. Stall characteristics on the airfoil elements were examined through plots of force, moment, and surface pressure data and flow visualization. Flap deflected configurations indicated a two-stage stall and hysteresis phenomenon. The hysteresis loop appeared to be a function of flap angle, gap geometry, and history of changes in air speed or angle of attack.

Nomenclature

C_d = drag coefficient
C_l = lift coefficient
$C_{l_{max}}$ = maximum lift coefficient
C_m = pitching moment coefficient
C_p = static pressure coefficient, $\equiv (p - p_\infty)/q_\infty$
c = mean chord, $\equiv 0.61$ m (2 ft) for the GA(W)-2 model
G/c = gap-to-chord ratio
O/c = flap overlap-to-chord ratio
p = local static pressure
p_∞ = freestream static pressure
q_∞ = indicated dynamic pressure, $\equiv 1150$ N/m^2 (24 psf)
x, y = airfoil coordinates: x is along the chord line
α = angle of attack
β = slot flow angle
δ = flap deflection angle

Introduction

MODERN aircraft wings are aerodynamically designed to operate within their performance limitations for a spectrum of conditions. Their flaps are retracted for cruise conditions and deflected at low speeds for high-lift generation during takeoff (to reduce takeoff distance), high $C_{l_{max}}$ and drag during landing (to reduce speed), and high lift-to-drag ratio during climbing (to reduce engine thrust). Within this spectrum, there should be a harmony between the interacting wing/flap components. This harmony provides the type of flowfield that is not in conflict with its boundaries, but has the same design point for both increasing and decreasing angles of attack. Any irreversibility in the airfoil performance needs to be known prior to the airfoil use for actual flight conditions. Considering the scale effects, this can be determined by wind-tunnel testing.

The few wind-tunnel test results reported in the literature show that a hysteresis loop occurs on the aerodynamic forces of single-element airfoils at low Reynolds numbers (below 700,000). These tests were made for either an airfoil placed between two-dimensional inserts,[1] preventing three-dimensional wing tip effects over the model, or a planform wing left free at the ends.[2-5] However, to get closer to the actual flight conditions, the tests should be conducted at high Reynolds numbers for not only single-element airfoil but also multielement airfoil configurations.

The present paper concentrates on force, moment, and surface pressure measurements for a test matrix of two-element airfoil while increasing and then decreasing angles of attack at a fixed high Reynolds number. Emphasis is placed on the complex flow mechanism and the associated hysteresis effects on separation characteristics around the airfoil elements. Flowfield quantities such as pressures and velocities were also measured for the same two-element airfoil.[6,7]

Experimental Arrangement

The tests were conducted in the Wichita State University (WSU) 2.13×3.05 m (7×10 ft) wind tunnel, which is a closed return tunnel with atmospheric test section static pressure. The tunnel is equipped with a pyramidal type balance that measures forces and moment with linearized wall corrections, as an average of 10 readings 0.2 seconds apart. The test model was mounted between two inserts, providing a 2.13 m (7 ft) high and 0.914 m (3 ft) wide two-dimensional test section,[8-10] as shown in Fig. 1.

The test model used was the 13%-thick GA(W)-2 airfoil with 25%-single-slotted flap, having a reference chord of 0.61 m (2 ft) at flap-nested position and a span of 0.914 m (3 ft). The main wing terminates at $0.875c$ and has a cove region where the flap retracts for the single-element case. The model was attached to the tunnel balance system through a set of 1.06 m (3.5 ft) diam aluminum end plates. The model pivot location was at $0.5c$ station. Along the midspan of the main wing and flap, there were 69 pressure taps available for the surface pressure measurements. The pressure taps connected to pressure transducers, having a resolution of ± 2.4 N/m^2 (0.05 psf). The transition on the main wing boundary layer was fixed by 2.4-mm-wide trip strips at $5\%c$ upper and $10\%c$ lower surface.

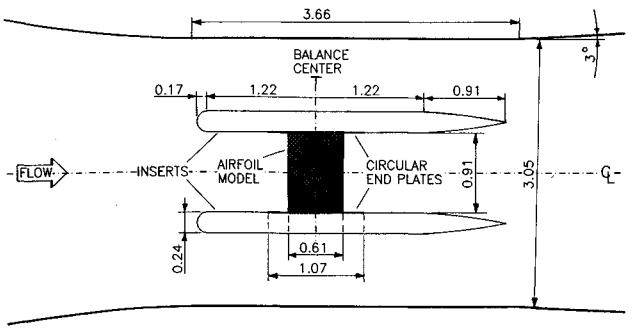

Fig. 1 WSU 7×10 ft wind tunnel with 7×3 ft two-dimensional inserts, m.

Presented in part as Paper 92-0267 at the AIAA 30th Aerospace Sciences Meeting, Reno, NV, Jan. 6-9, 1992; received March 16, 1992; revision received June 12, 1992; accepted for publication June 27, 1992.

*Postdoctoral Fellow, National Institute for Aviation Research. Member AIAA.

†Distinguished Professor, Department of Aerospace Engineering. Associate Fellow AIAA.

With the inclusion of the single-element airfoil, five different airfoil configurations, each having a different gap, were selected for the present experiments. However, in this paper, the results will be presented for typical test cases. Full results are available in Ref. 7 for the test matrix shown in Table 1. The selection of the test matrix was based on previous flap optimization studies[9] conducted for NASA at WSU on the GA(W)-2 airfoil, maximizing $C_{l_{max}}$. Figure 2 shows the geometric details of flap setting. Each flap deflected case (30 and 40 deg) had an optimum and a narrow gap. For the optimum gap, the main wing wake does not merge with the boundary layer on the flap upper surface until near the flap trailing edge, but stays adjacent.[11,12] The narrow gap, on the other hand, produces a confluent boundary layer a short distance downstream from the flap leading edge. The gap geometry may be described by the slot flow angle β shown in Fig. 2, more physically significant than flap overlap. It is the angle between the slot flow vector and the main wing chord line. The slot flow vector is normal to the minimum radius line from the wing trailing edge to the flap leading edge.

All wind-tunnel tests were conducted at Reynolds number, based on the reference chord, of 2.2×10^6, Mach number of 0.13, and an indicated dynamic pressure of 1150 N/m^2 (24 psf). The test section turbulence level was 1%, as obtained by a single hot-wire probe.

The flow two dimensionality in the test section was evaluated by the visualization of separation patterns on the model upper surface. Tempera and kerosene flow showed a change in two-dimensional flow character near the sidewalls with the airfoil stalled. Beyond the stall, a spanwise surface flow component within the separated zone appeared and extended toward the juncture of the model and sidewall, where a vortex pair formed and shed at the model trailing edge. However, this was limited to the outer 25% of the span. No boundary-layer control was employed to reduce the three-dimensional flow patterns. The sidewall boundary layer did not have significant effect on the airfoil stall characteristics.[8] This was probably due to the relatively short upstream length of the sidewalls, 1.06 m from the model leading edge. Besides tempera and kerosene, tufts were attached to the model upper surface to supplement the preceding results.

Results

Forces and Moment

Aerodynamic lift, drag, and pitching moment were measured for all test configurations using the tunnel balance and reduced to coefficient form as C_l, C_d, and C_m. The balance C_l values were compared with those produced by the integration of surface C_p values. Considering all test cases, the integrated C_l was very close to or at most 4% higher than the corresponding balance C_l. The results agree reasonably well with the Ref. 9 data, but the angle-of-attack range of the present tests, -8 deg to about 20 deg, is higher than the range in Ref. 9.

Results of these tests with optimum gaps are presented in Fig. 3. It is clear that deflecting the flap from nested position to 40 deg increases the C_l, but decreases the stall angle of attack. For 40 deg of flap deflection, there is an increase in lift slope just prior to stalling. This was also present in the Ref. 9 data. Flow visualization data confirmed that this was due to increases in the slot flow angle. The termination of the wing

Table 1 Test matrix

Cases	A	B	C	D	E
α, deg	10	0	0	0	0
	15	12.8	12.8	12.8	12.8
	20	15.5	15.5	15.5	15.5
δ, deg	0	30	30	40	40
β, deg	—	21	33	67	55
G/c	—	0.03	0.02	0.015	0.0115
O/c	—	0	0	−0.01	−0.007

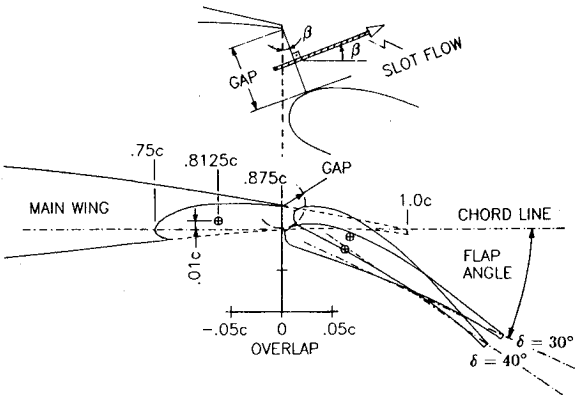

Fig. 2 Flap position and gap geometry for the GA(W)-2 airfoil.

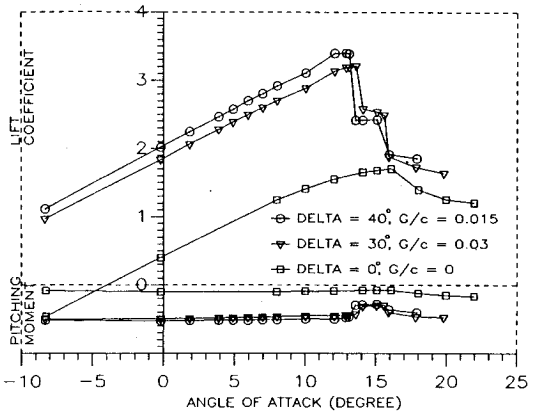

Fig. 3 Effect of flap setting on lift and moment coefficients.

trailing edge at 0.875c rather than 1.0c (12.5% cutout) reduced the so-called Coanda effect of the slot flow. Instead, it helped the slot flow act as an ejector on the wing trailing edge to diminish the effects of adverse pressure gradients.

After the stall, the flapped test cases show a sharp decrease in C_l and C_m and increase in C_d. The sudden loss of airfoil performance was accompanied by an abrupt change of flow pattern on the upper surface and a noticeable increase in model buffeting. Previously published test results have quit taking data after this abrupt stall. The present test results indicate nearly constant aerodynamic coefficients after this stall, as shown in Fig. 3. The higher the flap deflection, the larger the drop, and the wider the constant C_l line appears to be. Increasing the angle of attack caused another sharp drop on the lift curve. This interesting feature of the flap-deflected configurations was always present and is interpreted as a two-stage stall: stall on the flap and then stall on the wing.

Hysteresis Effects

Wind-tunnel studies of airfoil aerodynamics are of great importance for designing and building aircraft. Much work has been devoted to this field, but it appears that none of these studies are really concerned with the possible existence of hysteresis effects on multielement airfoils. Hysteresis has been considered as a low Reynolds number phenomenon, occurring in the poststall recovery of single-element airfoils. However, the present tests reveal that even at a relatively high Reynolds number, hysteresis may still affect the results of wind-tunnel testing. Here, these effects are presented, considering both the airfoil performance and surface pressures.

For the force and moment measurements, the model was set to 0-deg angle of attack at the wind-off conditions, and then the tunnel speed was increased to the one corresponding to the test Reynolds number. Once the tunnel stabilized, the angle of attack was decreased to -8 deg and then increased to about 20 deg while collecting data at prescribed angles of attack. After

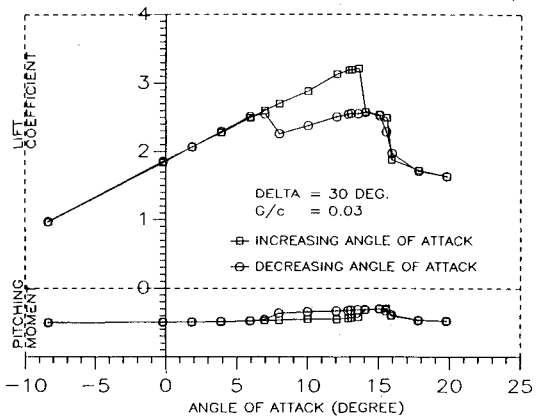

Fig. 4 Hysteresis effect on lift and moment coefficients for test case B.

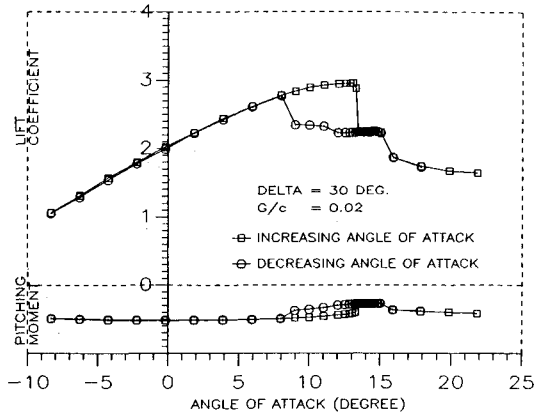

Fig. 5 Hysteresis effect on lift and moment coefficients for test case C.

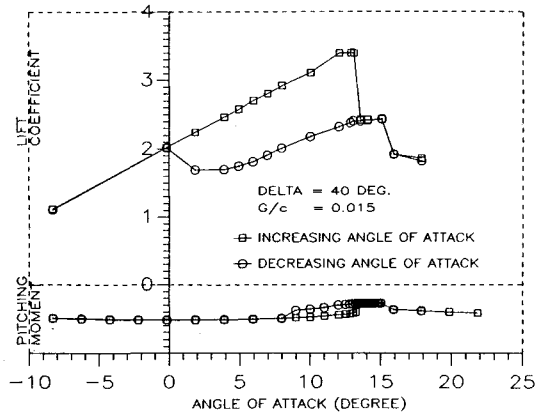

Fig. 6 Hysteresis effect on lift and moment coefficients for test case D.

its maximum value, the angle of attack was decreased back to −8 deg without stopping the tunnel.

The single-element airfoil case of the present tests did not experience any hysteresis loop despite the stall hysteresis effects seen on other single-element airfoils at relatively low Reynolds numbers (below 700,000), as reported in Refs. 1-5.

However, as the flap was deflected to 30 deg with optimum gap, there was a large hysteresis loop in the data. As seen in Fig. 4, about 20% of the $C_{l_{max}}$ is lost as the angle of attack is decreased below 14 deg. The loss of lift continues until the angle is decreased to 7 deg. There appears to be a downward shift in the lift curve between these two angles. It is known that the primary function of the flap is the opposite of what is happening in the lift curve. That is, the flap increases the $C_{l_{max}}$ by shifting the lift curve upward and in the negative angle-of-attack direction. But the present results show that whatever performance is gained by deflecting the flap is diminished or eliminated within the hysteresis loop. Narrowing the gap for the 30-deg flap angle reduced the size of the hysteresis loop, ranging from 8 to 13 deg, Fig. 5. This was attributed to about 12-deg increase in the slot flow angle and about 30% reduction in the gap width for the same flap angle and overlap.

The hysteresis effects were quite severe for the 40- deg flap with optimum gap, ranging from 0 to 13 deg, Fig. 6. This is due to relatively high slot flow angle, giving a large vertical component to the slot flow. Typical drag and drag polar curves of this test case are shown in Figs. 7 and 8, respectively. The hysteresis loop in the drag values has the same range of angle of attack as the lift curve.

Knowing the range of hysteresis loop from the force and moment data, surface pressures were measured for the study of stall characteristics on the flapped configurations. The selected angles of attack included the beginning, center, and termination of the hysteresis loop. As an example, for the

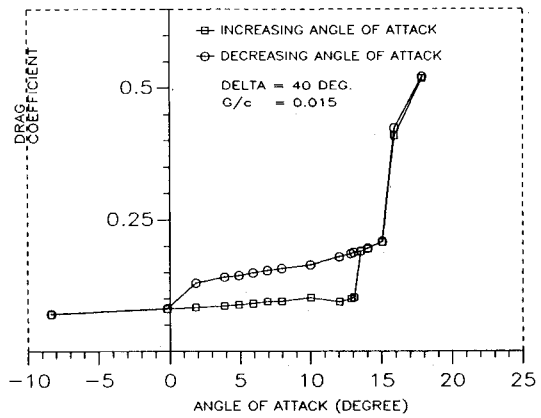

Fig. 7 Hysteresis effect on drag coefficient for test case D.

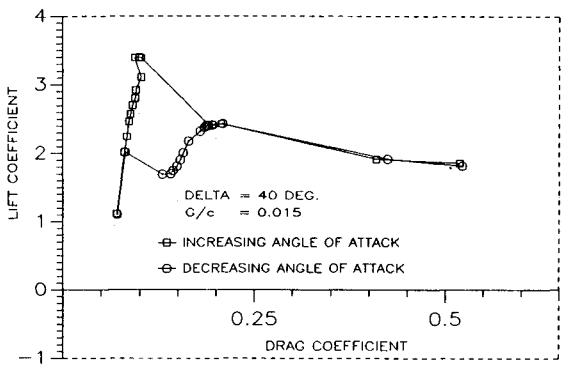

Fig. 8 Hysteresis effect on drag polar for test case D.

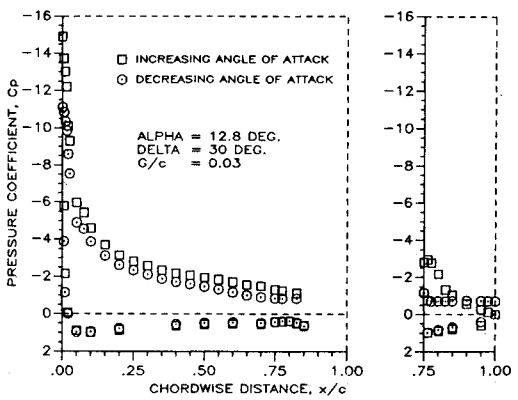

Fig. 9 Hysteresis effect on surface pressure distribution for test case B at α = 12.8 deg.

30-deg flap case with optimum gap, the surface pressure distribution was attained, first at $\alpha = 7$, 8, 12.8, 14, and 15.5 deg for the increasing side and then the reverse of these for the decreasing side of the lift curve. The results of this case indicated a discrepancy between the surface pressure distributions only within the hysteresis loop determined by the corresponding lift curve, as anticipated. The highest discrepancy occurred at $\alpha = 12.8$ deg, which is around the $C_{l_{max}}$ angle, as shown in Fig. 9. Considering the regions of constant pressures to be an indication of the flow separation, the flow on the flap upper surface is fully attached for the increasing side and fully detached for the decreasing side of the lift curve while the flow on the main wing is attached in both cases. These separation regions were also confirmed by surface flow visualization. However, the suction pressures on the main wing are lower for the decreasing case, because the flap does not provide the necessary downwash and, therefore, circulation for the wing as it does while increasing the angle of attack. This means that the hysteresis loop is primarily as a result of the change of flow pattern about the flap rather than the main wing.

As the angle of attack is increased to 14 deg or greater, the hysteresis effects disappear on the surface pressure distributions, Fig. 10. At $\alpha = 14$ deg, the flap is completely stalled and there is separation from the main wing trailing edge. The separation point moves upstream on the main wing upper surface as the angle of attack is increased to 15.5 deg, Fig. 11. It appears that this upstream movement of the separation point on the main wing corresponds to the flatness on the aerodynamics coefficients between 14 and 15.5 deg of angles of attack. These results clearly show that the stall on the flap is followed by the stall on the main wing.

Discussion

Considering the airfoil performance, the hysteresis loop appears to result from the flap deployment. The flow around the flap is very complex due to the interactions between different layers of the flow. The boundary-layer flow over the main wing is thick and turbulent for most of the wing. It separates at the wing trailing edge and extends over the flap as a wake with adverse pressure gradient at low angles of attack. On the other hand, the boundary layer over the flap is thin and laminar and tends to stay so due to the favorable pressure gradient and convex curvature. This favorable pressure gradient is provided by the slot flow passing through the gap. The flow is highly accelerated potential flow with low pressures compared to the neighboring flows. This low pressure region creates strong pressure gradients across the flow just above the flap.

The slot flow centerline, depicted as a vector in Fig. 2, tends to follow the flap curvature under the influence of strong pressure gradients in the wing wake and its angle increases with the angle of attack, influenced by the wing wake over the boundary layer on the flap. Since the wing wake is stronger, it pushes the flap boundary layer downward toward the surface,

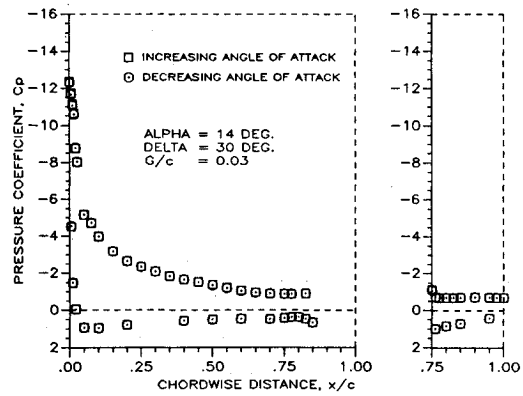

Fig. 10 Hysteresis effect on surface pressure distribution for test case B at $\alpha = 14$ deg.

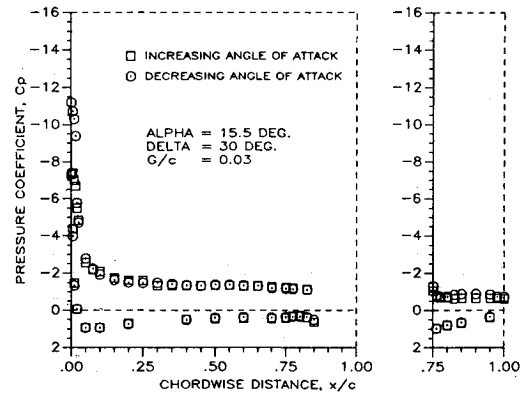

Fig. 11 Hysteresis effect on surface pressure distribution for test case B at $\alpha = 15.5$ deg.

limiting its ability for separation. This type of interaction continues until the stall angle. At the stall angle, the separating streamline at the wing trailing edge cannot resist the adverse pressure gradients and starts moving just upstream of the trailing edge. When this happens, the boundary layer on the flap becomes free of strong wake influence. It can now become thicker and stronger. It can even be separated with a slight increase of angle of attack. This is when the first abrupt stall occurs on the flap. In fact, the flap boundary layer always had the potential of separation before the wing boundary layer due to the flap deflection. But with the aid of the slot flow, the wing wake suppresses this potential until the stall.

After the first stall, the separating streamline moves farther upstream on the main wing. This is where there appears to be nearly constant aerodynamic coefficients as mentioned earlier. This steplike change in the C_l plots is short and terminates by the stall of the main element. Once both airfoil elements stall, there occurs a large separated region on the airfoil. The separated wing wake mixes with the separated boundary layer on the flap so that their separate identities no longer exist. This causes a big deficiency in the aerodynamic coefficients. To recover this deficiency, the airfoil model needs to pitch the nose down. The question here is whether the airfoil can gain the same $C_{l_{max}}$ that it had just before the first stall. There has not been a specific answer to this question in the current literature. One very obvious reason for this is the limitation on the maximum angle of attack in wind-tunnel testing due to buffeting. But a complete predictability of airfoil performance requires the knowledge of stall recovery and hence tests of this kind.

Although the main wing recovers from its stall and regains its part of the lift, the flap remains stalled to much lower angles of attack. Flat surface pressures on the flap show this. It seems that the flap loses its participation in the lift generation due to its uncambered effect after the stall. Also, once the flap becomes separated, its separated wake forms a bubble-shape region easily; that is, the flap shear layer combines with the separating streamline from the flap trailing edge at some distance downstream. Decreasing the angle of attack does not have much effect on the shape of the bubble, at least not as much as the flap deflection angle has on its formation. The rate at which this bubble decays is much slower for decreasing angle of attack than it is for increasing angle of attack. This is simply because once the wing wake and the flap boundary layer are both separated, they exchange momentum between each other for energy balance. The high momentum parts of wing wake are carried through the low momentum parts including the flap flow. A huge mixing takes place at different layers of the flow. Even though the geometric requirement of the conditions in which this mixing is created may be reversed precisely, dynamic changes of the wake are irreversible in nature. This process reduces the favorable effect of the slot flow on the flap upper surface and leaves the flap boundary layer separated until low angles of attack.

The hysteresis effects on the aerodynamic coefficients show that the hysteresis loop for the 40-deg flap case with optimum gap is the first and 30-deg flap case with optimum gap is the second largest of all tested configurations. This means that the flap setting plays an important role in the irreversibility of the flow. High flap deflections have higher potential of holding a separated bubble for longer time whenever its conditions are present. This potential becomes more readily available if there is a gap large enough to provide larger slot flow. In other words, the slot flow angle with the freestream flow and its gap width determines the level of hysteresis.

It was first thought that this hysteresis may not be present in three-dimensional testing or in actual flight conditions, but only for two-dimensional low aspect ratio flows. The tip vortex of a wing may assist the flow reattachment and the effect may ripple along the span. However, the hysteresis effects reported for wings at low Reynolds numbers raise a question about hysteresis even on full wing configurations.

Hysteresis may occur during wind-tunnel testing in a second way. In this occurence, the angle of attack is set at less than the one for $C_{l_{max}}$ at a given flap angle at wind-off condition, and then the tunnel speed is increased to that corresponding to the test Reynolds number. Once the flow settles down in the tunnel, the measurements can be made. However, the results may correspond to the lower side of the hysteresis loop obtained by changing the angle of attack at fixed tunnel speed. The flap stalls easily at low tunnel speeds and fails to attach as the air speed increases. Increasing Reynolds number from zero to the test value for a fixed angle of attack alters the boundary layer and associated separation characteristics. Initially, the boundary layer is laminar and it separates from the leading edge. As the tunnel speed increases continuously, the separation point tends to move downstream, but at a rather slower rate than if it was moving from the trailing edge to leading edge, as in the case of increasing angle of attack. At the test Reynolds number, the separation point reaches its final location on the airfoil upper surface, but that location is upstream of the separation point produced by the angle-of-attack changes. Those who test multielement airfoil configurations should be aware of this phenomenon.

Conclusions

1) The airfoil performance data show that the stall phenomenon occurs in two stages for the flap extended configurations. The first stall occurs on the flap and the second one on the main wing. Both are rather abrupt. This feature of multi element airfoils has probably not been reported by previous investigators, because they have quit taking data after the first stall.

2) Airfoil performance was determined in a loop of increasing and then decreasing angles of attack. The data show a large hysteresis loop for the flap extended configurations. The hysteresis effects appear to be a function of flap angle, gap geometry, and history of changes in air speed or angle of attack.

3) The surface pressure measurements conducted for the hysteresis study also confirm that the flow first separates from the flap and then progresses on the main wing.

References

[1]Satran, D., and Snyder, M. H., "Two-Dimensional Tests of GA(W)-1 and GA(W)-2 Airfoils at Angle-of-Attack from 0 to 360 Degrees," Wichita State Univ., Wind Energy Rept. 1, Wichita, KS, Jan. 1979.

[2]Winkelmann, A. E., "An Experimental Study of Separated Flow on a Finite Wing," AIAA Paper 81-1882, Aug. 1981.

[3]Marchman, J. F., III, and Abtahi, A. A., "Aerodynamics of an Aspect Ratio 8 Wing at Low Reynolds Numbers," *Journal of Aircraft,* Vol. 22, No. 7, 1985, pp. 628–634.

[4]Marchman, J. F., III, and Abtahi, A. A., "Effects of Aspect Ratio on Stall Hysteresis for the Wortmann Airfoil," AIAA Paper 85-1770, Aug. 1985.

[5]Marchman, J. F., III, and Sumantran, V., "Acoustic and Turbulence Influences on Stall Hysteresis," AIAA Paper 86-0170, Jan. 1986.

[6]Biber, K., and Zumwalt, G. W., "Flowfield Measurements on a Two-Element Airfoil with Large Separation," *AIAA Journal* (to be published).

[7]Biber, K., "Experimental Study of A Two-Element Airfoil with Large Separation," Ph.D. Dissertation, Wichita State Univ., Wichita, KS, Nov. 1991.

[8]Wentz, W. H., Jr., and Seetharam, H. C., "Development of a Fowler Flap System for a High Performance General Aviation Airfoil," NASA CR-2443, Dec. 1974.

[9]Wentz, W. H., Jr., "Wind Tunnel Tests of the GA(W)-2 Airfoil with 20% Aileron, 25% Slotted Flap, 30% Fowler Flap and 10% Slot-Lip Spoiler," NASA CR-145139, 1977; also Wichita State Univ., Aeronautical Report 76-2, Wichita, KS, Aug. 1976.

[10]Wentz, W. H., Jr., and Fisko, K. A., "Pressure Distributions for the GA(W)-2 Airfoil with 20% Aileron, 25% Slotted Flap and 30% Fowler Flap," NASA CR 2948, Feb. 1978.

[11]Foster, D. N., Irwin, H. P. A., and Williams, B. R., "The Two-Dimensional Flow Around A Single-Slotted Flap," Royal Aeronautical Establishment, R&M 3681, Farnborough, England, UK, Sept. 1971.

[12]Smith, A. M. O., "High-Lift Aerodynamics," *Journal of Aircraft,* Vol. 12, No. 6, 1975, pp. 501–530.